



Effects of Quenching Temperature and Cooling Rate on the Microstructure and Mechanical Properties of U75V Rail Steel

Yuzhe Lan^{1,2} · Gang Zhao^{1,2} · Yaowen Xu^{1,2} · Chuanlong Ye^{1,2} · Shaocheng Zhang^{1,2}

Received: 14 June 2018 / Revised: 12 January 2019 / Accepted: 5 February 2019 / Published online: 22 February 2019
© ASM International 2019

Abstract

In order to investigate the effects of quenching temperature and cooling rate on the microstructure and mechanical properties of the U75V rail steel, Gleeble-3500 thermal simulator and tensile tester were applied and the dynamic CCT curves were obtained. The results show that low quenching temperature of 750 °C narrows the range of the cooling rate of only pearlite transformation, and the pearlite interlamellar spacing decreases with an increase in the cooling rate or the quenching temperature in this range. The minimum value of the pearlite interlamellar spacing is found to be 0.101 μm. At three quenching temperatures of 810, 780, and 750 °C, the microhardness increases with an increase in the cooling rate. In addition, the starting transformation temperature from austenite to pearlite does not exceed 700 °C, and the end temperature does not drop below 500 °C. The mechanical properties including yield strength, tensile strength, and total elongation of the selected specimens are improved as the pearlite interlamellar spacing decreases and meet the requirements. For the field production of the U75V rail steel, higher quenching temperature and a cooling rate of 3–5 °C/s are the best choices.

Keywords Gleeble-3500 thermal simulator · Quenching temperature · Cooling rate · Pearlite interlamellar spacing · Mechanical properties · U75V rail steel

Introduction

It is observed that the quality of traction, speed of driving, density of transportation, and the annual total weight have been greatly improved with the development of the railway industry in China [1]. These factors significantly increase

the load on and damage to the rail. Therefore, it is necessary to improve the rail strength and the wear resistance of rail to prolong its service life. In order to improve the rail strength, both heat treatment and alloying can be used, but over the years the results of research and application show that heat treatment is superior to alloying because of its low cost and high efficiency, and heat treatment can also extend the service life of heavy rail at least one more time [2]. Heat treatment has been developed from tempering (Q-T) to slack quenching (S-Q) [3] and finally online heat treatment.

The quenching temperature and cooling rate significantly affect the microstructure and mechanical properties of the heavy rail U75V steel in the cooling process of the rail. The major research studies have primarily focused on the temperature distribution and phase transition in the cooling process by using the finite-element modeling (FEM) method [4–10]. Generally, the rail steel can be directly treated by online heat treatment after universal rolling. The recent studies have paid close attention to the dynamic continuous cooling transformation (CCT) curve or the time–temperature–transformation (TTT) curve of the U75V steel, which has emerged out of the universal rolling mill [11–19]. In fact, some steel mills have faced difficulties because of a

✉ Yaowen Xu
xuyw@wust.edu.cn

Yuzhe Lan
892354593@qq.com

Gang Zhao
zhaogang@wust.edu.cn

Chuanlong Ye
yechuanlong@wust.edu.cn

Shaocheng Zhang
1165010835@qq.com

¹ Key Laboratory for Ferrous Metallurgy and Resources Utilization of Ministry of Education, Wuhan University of Science and Technology, Wuhan 430081, China

² Hubei Provincial Key Laboratory for New Processes of Ironmaking and Steelmaking, Wuhan University of Science and Technology, Wuhan 430081, China

distance between the quenching unit and the universal rolling export. Obviously, the temperature of the rail decreases when the U75V steel reaches the quenching unit. It is essential to examine whether the quenching scheme provided by the major research studies meets the requirements of the microstructure and properties of the U75V rail steel.

Therefore, the objective of this study was to investigate the microstructure and properties of the heavy rail U75V steel after unconventional online heat treatment, including the pearlite interlamellar spacing, microhardness, and dynamic CCT curve. Furthermore, to obtain elongation, yield strength, and tensile strength, the tensile test of the finished steel was carried out, which provides theoretical guidance for field production.

Experimental Procedure

Thermal Simulation Experiments

In this study, experimental materials were taken from U75V rail billet. The chemical composition (in mass percent, %) was as follows: C 0.71–0.80, Si 0.50–0.80, Mn 0.70–1.05, S \leq 0.030, P \leq 0.030, V 0.04–0.12, and Nb \leq 0.010. These materials were processed into 27 cylindrical specimens, and their respective shapes are shown in Fig. 1. Rolling deformation was simulated by using single-pass axial compression in the Gleeble-3500 thermal simulator (DSI, New York, NY, USA). First, all the specimens were austenitized at 1200 °C for 5 min at a heating rate of 5 °C/s and cooled to 890 °C at a rate of 3 °C/s, held for 5 s to a uniform temperature, and then compressed for 50% and 1 s⁻¹. After deformation, the specimens were cooled to 810, 780, and 750 °C at 1 °C/s, respectively, and finally cooled to room temperature at nine different cooling rates of 0.1, 0.5, 1, 2, 3, 5, 7, 10, and 15 °C/s, respectively. Figure 2 presents the specific process scheme.

Microstructure Examinations and Tensile and Hardness Tests

In order to obtain the pearlite interlamellar spacing, after thermal simulation experiments, a Nova 400 Nano

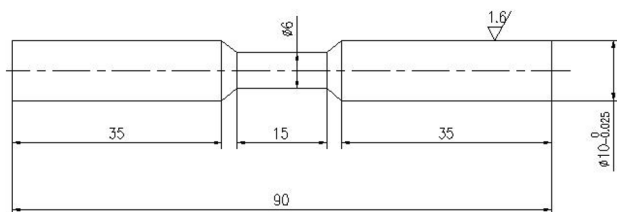


Fig. 1 Dynamic CCT sample size of the U75V rail steel (all dimensions are in mm)

scanning electron microscope (SEM; FEI, Hillsboro, OR, USA) and an optical microscope were used to examine the microstructures of the simulated specimens. An HV-1000B Vickers hardness tester (with a load of 0.98 N) was used to measure the Vickers microhardness. In order to calculate average values, each specimen was assigned ten points for the microhardness test. In addition, to conduct tensile tests and to study the elongation, yield strength, and tensile strength, we selected the specimens that fulfilled the hardness requirement of TB/T 2344-2012 [20]. Table 1 presents the names of the selected specimens.

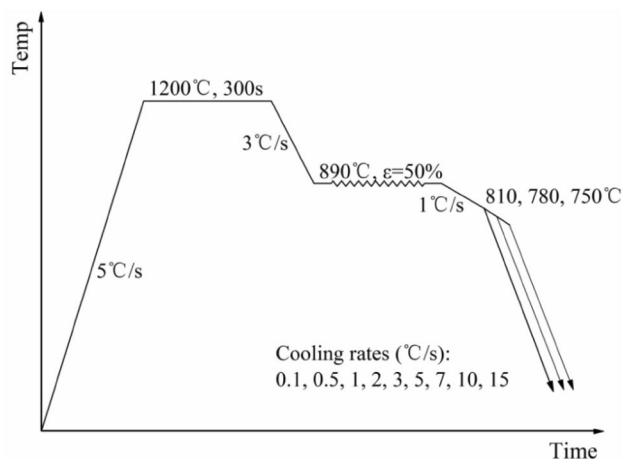


Fig. 2 The online heat treatment process of the heavy rail U75V

Table 1 Notations and cooling parameters of specimens

Specimen	Quenching temperature, °C	Cooling rate, °C/s
A	As-cast condition	As-cast condition
B	750	3
C	780	3
D	780	5
E	810	1
F	810	5

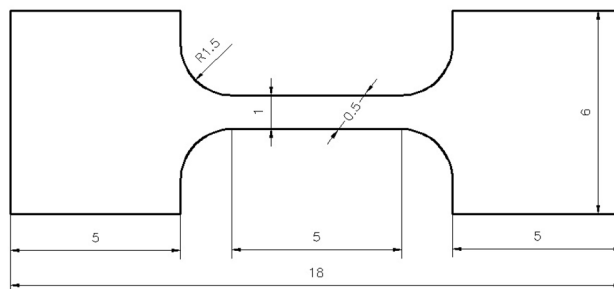
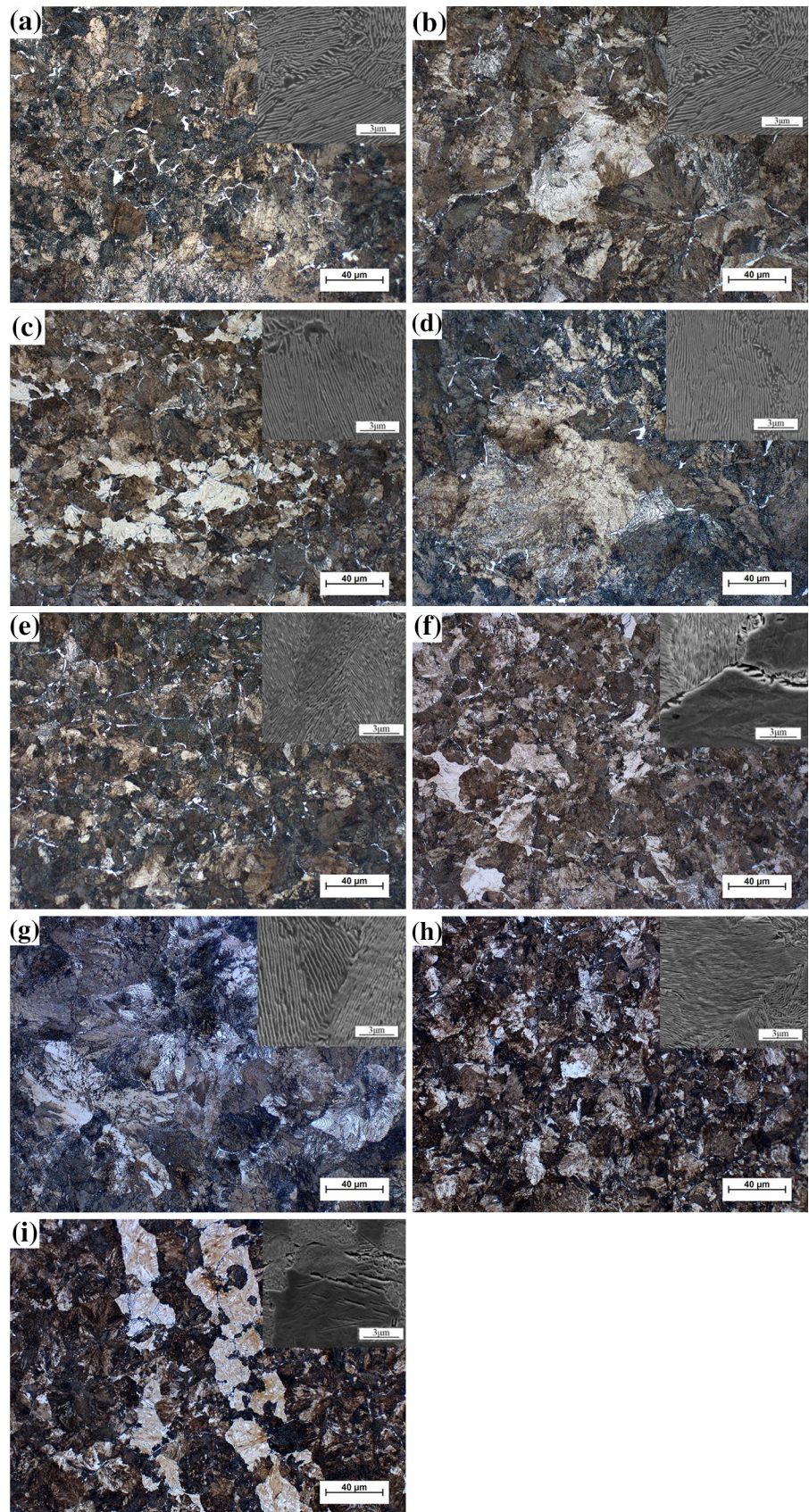


Fig. 3 U75V steel microtensile specimen size (all dimensions are in mm)

Fig. 4 Microstructures of U75V steel at different cooling conditions: (a, b, c) 750 °C; (d, e, f) 780 °C; (g, h, i) 810 °C; (a, d, g) 0.1 °C/s; (b) 3 °C/s; (c, e, h) 5 °C/s; (f, i) 7 °C/s



A UTN-4503 electronic universal tensile tester (SUNS, Shenzhen, China) with a crosshead speed of 1 mm/min at room temperature was used to carry out the tensile tests. The tensile specimen size is shown in Fig. 3. For each specimen, three tensile tests were repeated and the corresponding average values were calculated.

Results and Analysis

Microstructures and Microhardness

Figure 4 shows the partial microstructures of the U75V steel at different quenching temperatures and cooling rates. These microstructures contain ferrite, lamellar pearlite, and martensite. It is observed that only pearlite transformation occurs at a cooling rate of 0.1–3 °C/s and martensite emerges at a rate of 5 °C/s when the quenching temperature is 750 °C. However, martensite emerges at a rate of 7 °C/s when the quenching temperature is 780 and 810 °C. Martensite is resolutely unable to appear in the rail because of its poor wear resistance, which indicates that high quenching temperature is advantageous for the formation of pearlite.

The pearlite interlamellar spacing of the U75V rail steel under different cooling conditions is shown in Fig. 5. The relationship between the pearlite interlamellar spacing and the supercooling degree in the carbon steel can be expressed as follows [21, 22]:

$$s = 8.02 \times 10^{-4} / \Delta T \quad (1)$$

where s is the pearlite interlamellar spacing and ΔT is the supercooling degree. The above empirical formula indicates that s varies inversely with ΔT , which means in the case of pearlitic transformation the pearlite interlamellar spacing reduces with an increase in the supercooling degree. As the supercooling degree increases with an increase in the cooling rate, the transformation temperature from austenite to pearlite decreases and the distance of diffusion of elements reduces. Accordingly, the pearlite interlamellar spacing is reduced with an increase in the cooling rate. Figure 5 shows that, as verified by the above formula, the pearlite interlamellar spacing decreases with an increase in the cooling rate at three quenching temperatures of 750, 780, and 810 °C. When only pearlite transformation occurs, the minimum value of the pearlite interlamellar spacing is found to be 0.101 μm. When the quenching temperature is 750 °C, the pearlite interlamellar spacing at 5 °C/s is not displayed, which is an exception. At that point, martensite transformation has already been started, and then the pearlite sheets are stuck together even granulated to not be distinguished. Furthermore, it is observed that higher quenching temperature can obtain much better fine pearlite interlamellar spacing at the same cooling rate.

In addition, Fig. 6 shows the microhardness values of the U75V rail steel under different cooling conditions. The performance of steel depends on the microstructure. For example, at a quenching temperature of 810 °C, the cooling rate changes from 0.1 to 5 °C/s, and mainly pearlite is obtained and the hardness increases slowly from HV 329 to HV 392. When the cooling rate is greater than 7 °C/s, the microstructure emerges as a result of martensite, and the microhardness further increases. When the cooling rate is 15 °C/s, the maximum hardness reaches HV 687. The microhardness increases with an increase in the quenching temperature at the same cooling rate. The pearlite interlamellar spacing plays the most important role at a lower cooling rate. However, the amount of martensite makes a difference at a

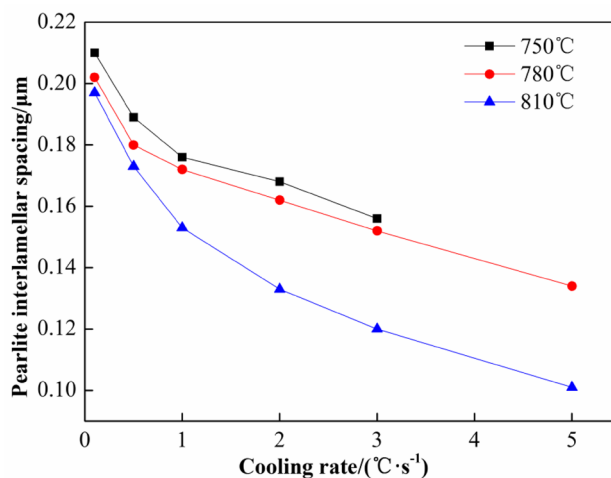


Fig. 5 Pearlite interlamellar spacing of the U75V rail steel under different cooling conditions

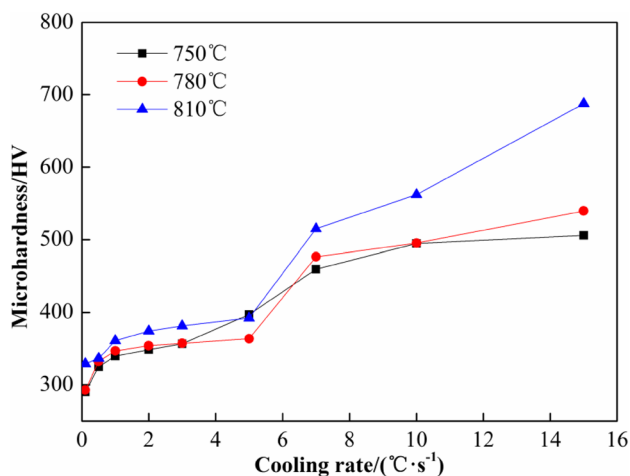


Fig. 6 Microhardness values of U75V rail steel at different cooling conditions

higher cooling rate. The latter at 750 °C defeats the former at 780 °C at a cooling rate of 5 °C/s.

Dynamic CCT Curves

By using a Gleeble-3500 thermal simulating test machine, it is observed that the expansion curve varies with temperature when the cooling rate is 5 °C/s as shown in Fig. 7a. The tangent method is used to determine the phase transition beginning temperature (610 °C) and the phase transition end temperature (525 °C). Similarly, all temperature points are determined for each cooling rate, and the dynamic CCT curves at three different quenching temperatures of the steel are shown in Fig. 6b–d, respectively, which are the results of phase transformation measurement and microstructure

observation. Figure 7b, c, and d shows that the products of austenite transformation contain pearlite or sorbite at any quenching temperature and cooling rate. The starting transformation temperature from austenite to pearlite does not exceed 700 °C, and the end temperature does not drop below 500 °C. It is observed that martensite appears when the cooling rate is greater than 5 °C/s, and even when the quenching temperature is 750 °C and the cooling rate is 5 °C/s. The carbon content of the U75V rail steel is around 0.75%, and the theoretical eutectoid point moves left because of the additions of silicon, manganese, and vanadium [23]. In addition, from microstructures in Fig. 4, it can be seen that not only pearlite emerges but also ferrite emerges at low cooling rates and bainite appears around martensite at high cooling rates, which are not shown in the dynamic CCT curves. The

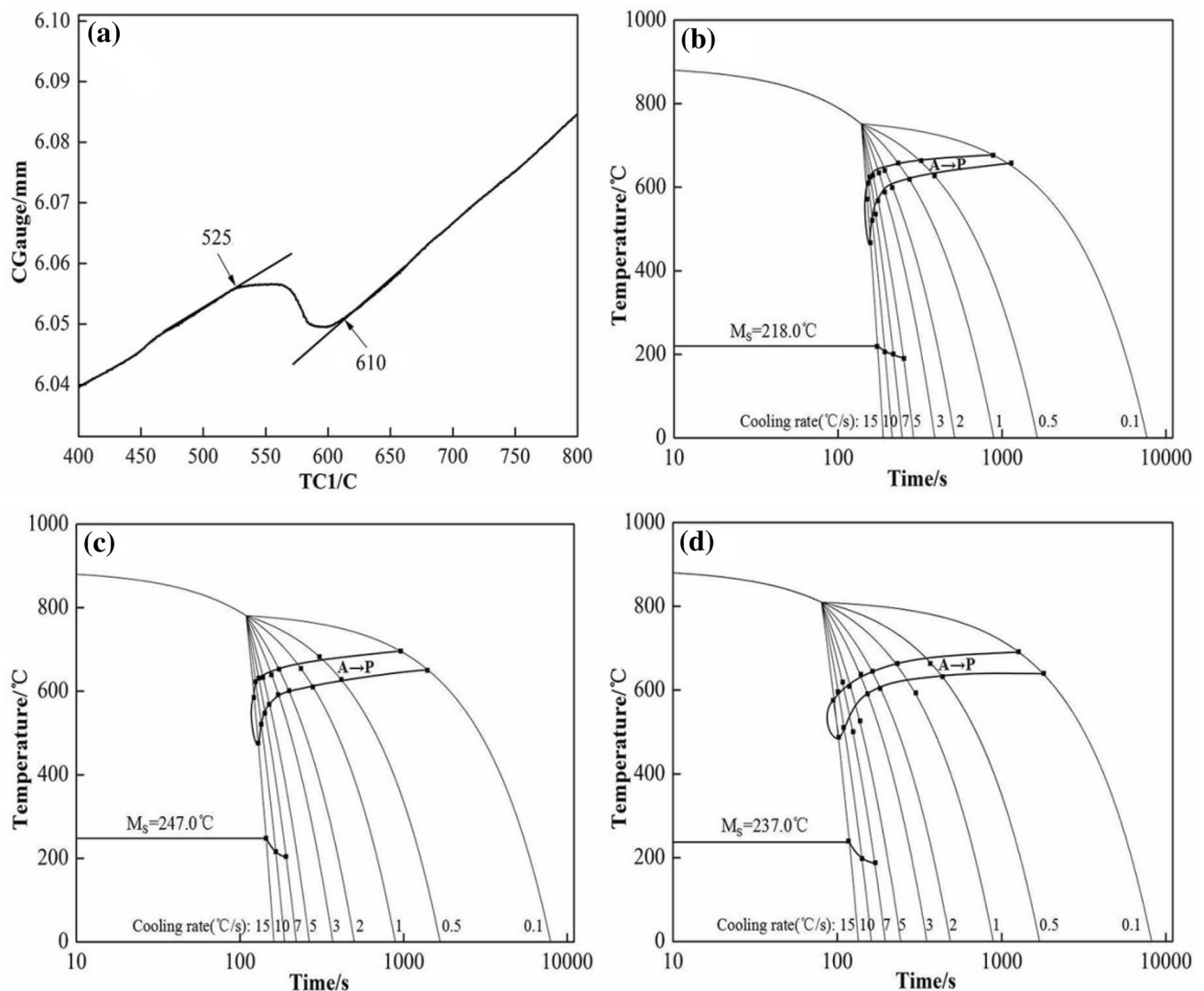


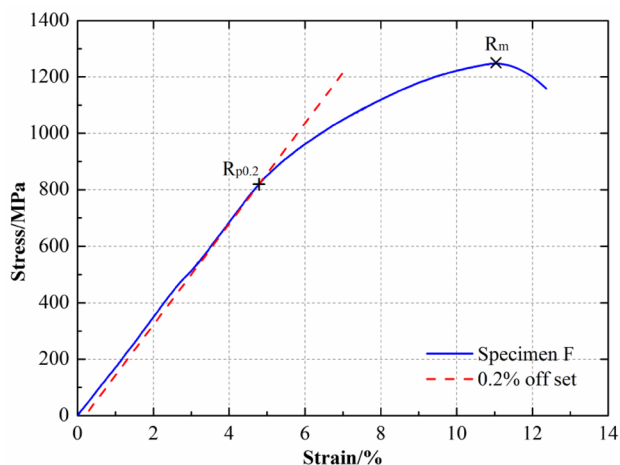
Fig. 7 (a) Expansion curve and phase transition temperature at 810 °C and 5 °C/s; dynamic CCT curves at three quenching temperatures: (b) 750 °C; (c) 780 °C; and (d) 810 °C

Table 2 Heat-treated rail tensile strength, elongation after fracture, and top strength of rail head

Steel grade	Yield strength, MPa	Post-break elongation A, %	Center line hardness of the top surface of the rail head HBW (HBW 10/3000)
U75V	≥ 1180	≥ 10	340–400

Table 3 The mechanical properties of the selected specimens

Specimen	Yield strength, MPa	Tensile strength, MPa	Total elongation, %
A	623	981	10
B	813	1204	11
C	818	1209	12
D	835	1217	11
E	816	1206	12
F	896	1225	12

**Fig. 8** The engineering strain–stress curve of the selected specimen after quenching. R_{eL} , yield strength; R_m , tensile strength

products of ferrite and bainite are due to the non-uniform distribution of carbon, which is not sufficient to reflect in the CCT curves.

Mechanical Properties

GB TB/T 2344-2012 43–75 kg/m rail ordering technical conditions for the performance of U75V steel including tensile strength, elongation after fracture, and hardness have a clear range of indicators as shown in Table 2.

Figure 8 shows the engineering strain–stress curve of the specimen after quenching at a temperature of 810 °C and a cooling rate of 5 °C/s. The yield strength with the stress value of the 0.2% residual deformation and the tensile strength with the resistance of the material with maximum uniform plastic deformation are obtained. Table 3 presents the tensile results of the selected specimens. When the interlamellar spacing is less than 0.156 μm , the tensile strength, total elongation, and microhardness of the rail steel meet the requirements of TB/T 2344-2012 as compared with the pearlite interlamellar spacing shown in Fig. 5. The maximum values of the tensile strength and total elongation are found to be 1225 MPa and 12%, respectively. Furthermore, the mechanical properties,

including yield strength, are improved with a decrease in the pearlite interlamellar spacing. In addition, ferrite and cementite become thinner, and the amount of phase interface can be increased and the ability of resisting the plastic deformation can be enhanced. On the other hand, the thinner cementite makes plastic deformation easier as compared to fracture [24, 25].

To summarize, the refinement of the pearlite interlamellar spacing improves not only the pearlite intensity but also plasticity, which is the theoretical basis of strengthening of heat treatment and toughening of rails. Finally, considering all observations, it is concluded that the quenching temperature should be increased as far as possible to obtain pearlite with fine interlamellar spacing. Furthermore, when the temperature of the quenching unit is increased as high as possible, the range of the cooling rate becomes wider, which helps in meeting the requirements of the rail steel and achieving excellent performance. Therefore, it is extremely important for the rail steel to preserve heat between the quenching unit and the universal rolling export. Therefore, if the quenching temperature floats up and down, a cooling rate of 3–5 °C/s may be a better choice.

Conclusions

1. The decrease in the quenching temperature narrows the range of the cooling rate of only pearlite transformation. Martensite, which appears at a cooling rate of 7 °C/s with quenching temperatures of 810 and 780 °C, appears at a cooling rate of 5 °C/s with a quenching temperature of 750 °C. The pearlite interlamellar spacing decreases with an increase in the cooling rate at the same quenching temperature. Similarly, it decreases with an increase in the quenching temperature at the same cooling rate.
2. The mechanical properties of the U75V steel are improved with a decrease in the pearlite interlamellar spacing. The tensile strength, total elongation, and hardness meet the requirements of the U75V rail steel when the pearlite interlamellar spacing is less than 0.156 μm .
3. The quenching temperature should not be reduced beyond a certain limit. It is observed that if the quench-

ing temperature floats up and down, a cooling rate of 3–5 °C/s is the best choice.

References

1. W. Zhong, J.J. Hu, Z.B. Li, Q.Y. Liu, Z.R. Zhou, A study of rolling contact fatigue crack growth in U75V and U71Mn rails. *Wear* **271**, 388–392 (2010)
2. H. Kang, D. Wu, X.M. Zhao, Surface temperature change of U75V 60 kg/m heavy rail during heat treatment. *J. Iron. Steel Res. Int.* **20**(2), 33–37 (2013)
3. H. Kang, Y.H. Wang, D. Wu, X.M. Zhao, Y.M. Wang, Research on quenching equipment of rail head. *Adv. Mater. Res.* **145**, 313–316 (2011)
4. J.G. Lenard, A study of temperature distribution in rails during intermittent cooling. *J. Mater. Process. Technol.* **25**, 303–320 (1991)
5. L. Chen, F. Zhang, Z.Y. Zhang, R. Wei, Organization simulation analysis of the U75V cooling process. *J. Metall. Eng.* **3**(1), 48–51 (2014)
6. M.X. Gao, H. Jia, J.J. Jiang, P.L. Wang, H. Song, S.Y. Yuan, Z.Q. Wang, The effect of initial cooling temperature on deformation of U75V heavy rail after cooling. *Adv. Eng. Forum* **2–3**, 667–672 (2011)
7. J. Basu, S.L. Srimani, D.S. Gupta, Rail behaviour during cooling after hot rolling. *J. Strain Anal. Eng.* **39**(1), 15–24 (2004)
8. S.L. Srimani, J. Basu, Nonlinear analysis of residual stresses in a rail manufacturing process by FEM. *J. Strain Anal. Eng.* **38**, 261–268 (2003)
9. G. Li, H.Y. Cui, Analysis of 100-meter rail temperature field during cooling process before straightening by FEM. *Int. J. Mod. Phys. B* **23**(6&7), 1203–1208 (2009)
10. M.X. Gao, H. Song, H. Jia, J.J. Jiang, S.H. Tong, S.Y. Yuan, Z.Q. Wang, Study on the temperature changing rules of U75V rail in the cooling process. *Proc. Eng.* **15**, 4579–4584 (2011)
11. H. Kang, X.M. Zhao, D. Wu, Effect of air pressure on hardened layer of U75V 60 kg/m heavy rail after heat treatment. *J. Harbin Inst. Technol. (New Ser.)* **20**(1), 52–56 (2013)
12. A.C. Ren, Y. Ji, G.F. Zhou, Z.X. Yuan, B. Han, Y. Li, Hot deformation behavior of V-microalloyed steel. *J. Iron. Steel Res. Int.* **17**(8), 55–60 (2010)
13. Y. Liu, Experimental investigation of the mechanical properties of quenched rails for different quenching conditions using the temperature directly from rolling heating. *J. Mater. Process. Technol.* **63**(1), 542–545 (1997)
14. R.Z. Luo, Study on dynamic CCT curve of U71Mn steel. *Zhejiang Metall.* **2**, 38–40 (2013). (in Chinese)
15. Y.G. Wang, Y.L. Ma, B.F. Wang, Study on CCT curve determination and continuous cooling transformation of U71Mn steel. *J. Baotou Univ. Iron Steel Technol.* **14**(3), 40–44 (1995). (in Chinese)
16. J.G. Zhang, X.G. Jing, TTT and CCT curve and microstructure analysis of U75V rail after induction heat treatment. *Hot Work. Technol.* **39**(8), 168–170 (2010). (in Chinese)
17. A.C. Ren, Y. Ji, L.Q. Zhao, Phase transformation behavior of U75V steel under continuous cooling. *Mater. Mech. Eng.* **32**(7), 15 (2008). (in Chinese)
18. B. Li, G.M. Zhu, G.M. Tao, Dynamic CCT curve of U75V steel for high-speed railway. *J. Iron Steel Res.* **26**(11), 20–24 (2014). (in Chinese)
19. B. Li, G.M. Zhu, G.M. Tao, Effect of online slacking-quench on the microstructure and properties of U75V rail. *Iron Steel* **49**(7), 101–193 (2014). (in Chinese)
20. Ministry of Railways of China, Rail ordering technical conditions. TB/T2344-201243 (2012). (in Chinese)
21. A.R. Marderand, B.L. Branefitt, The effect of morphology on the strength of pearlite. *Metall. Trans.* **7**, 365–372 (1976)
22. Q.Y. Zhou, Y.H. Zhang, *Properties and Related Process of Rail* (China Railway Publishing House, Beijing, 2005). (in Chinese)
23. J.M. Hyzak, I.M. Bernstein, The role of microstructure on the strength and toughness of fully pearlitic steels. *Metall. Trans. A* **7**(8), 1217–1224 (1976)
24. K. Han, G.D.W. Smith, V. Edmonds, Pearlite phase transformation in Si and V steel. *Metall. Mater. Trans.* **26**(7), 1617–1631 (1995)
25. J. Ahmadi, M. Monirvaghefi, M. Salehi, Effect of pearlite interlamellar spacing on predominant abrasive wear mechanism of fully pearlitic steel. *Trans. Mater. Heat Treat.* **25**(5), 1207–1213 (2004)

Publisher's Note Springer Nature remains neutral with regard to jurisdictional claims in published maps and institutional affiliations.